Supporting information for

Deactivation/Activation of Quenching Defects in $CH_3NH_3PbI_3$ Perovskite by Direct Electron Injection/Extraction

Yu Du,[1] Sushu Wan[1], Yanghang Pan,[1] Mingyi Xie,[1] Mengning Ding,[1] Daocheng Hong,[2,*] and Yuxi Tian[1,*]

[1]*Key Laboratory of Mesoscopic Chemistry of MOE, School of Chemistry and Chemical Engineering, Nanjing University, Nanjing, Jiangsu, 210023, China*

[2] *Key Laboratory for Advanced Technology in Environmental Protection of Jiangsu Province, Yancheng Institute of Technology, Yancheng, Jiangsu, 224051, China*

1. Experimental methods.

Sample preparation. Gold electrodes were deposited via electron beam evaporation platform (PVD75 Proline EB, Kurt J. Lesker) and laterally distributed on a glass substrate with a thickness of approximately 150 nm. For $CH_3NH_3PbI_3$ sample fabrication, 0.159 g CH_3NH_3I (Xi'an Polymer Light Technology Corp) and 0.461 g PbI_2 (Alfa Aesar) were dissolved in 1 mL γ-butyrolactone (Aladdin) by stirring at 80℃ for 60 min to prepare the stock solution. The crystals studied in this work were prepared by directly drop casting 30 μL $CH_3NH_3PbI_3$ solution in three times on a glass slide covered with gold electrodes following an annealing process for 10 min at 80℃.

PL measurements. The PL measurements were conducted on a home-built wide-field microscope based on Olymplus IX73 with excitation at 532 nm from CW diode laser. The luminescence signal was collected by a dry objective lens (Olympus LUCplanFI 40×, NA=0.6) and detected by an EMCCD camera (Andor Ixon U888) after passing through a 550 nm long-pass filter (ET550lp, Chroma). The excitation power density was 4.5 W/cm^2. The PL traces were measured by taking movies consisting of 400 - 500 frames and the exposure time per image was 100 ms. A transmission grating (Newport, 150 lines/mm) was put in front of the camera for the spectra measurement. PL lifetime measurements were carried out by using a single photon counting system (TCSPC, picoharp 300) with 532 nm excitation light from super continuous laser (Fianium SC-400). Voltage was applied by an external power supply. To ensure the comparability of data, the same area was chosen for different voltage and excitation power magnitude. Each new analysis area underwent a 5 min light soaking for

reaching a stable initial state before measurement. All the measurements were performed under ambient condition.

Current measurements and SEM characterizations. Current measurements were performed on the whole structure and detected by measurement unit from Agilent B2902A. SEM characterizations were performed on a Hitachi S-4800 instrument.

2. Scheme of laterally structured sample

To investigate the interactions between external voltage and $CH_3NH_3PbI_3$ crystals, a lateral structure as shown in Figure S1 was designed. The distance between two electrodes was about 45 μm. The $CH_3NH_3PbI_3$ single crystal in the size of micrometers was on top of the gap and connected with the two electrodes.

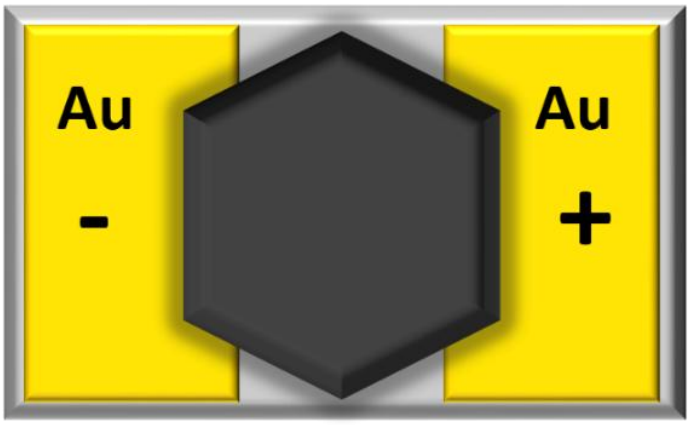

Figure S1. Schematic of laterally structured sample with a $CH_3NH_3PbI_3$ layer on the top. The test structure consisted of a symmetric 150 nm thick gold electrodes and 45 μm electrode gap distance on a glass substrate.

3. Rate constants of the PL enhancement and quenching during the voltage period ON and OFF

We also investigated the relationship between the rise/drop rate constants (Figure S2) in Figure 1d and observed similar time constants. Actually, in some regions, the rise processes during the voltage ON period was faster than the drop processes during the voltage OFF period while in some regions also showed opposed results as shown in Figure S3. And the time constants of these processes are fitted and listed in Table S1 and S2.

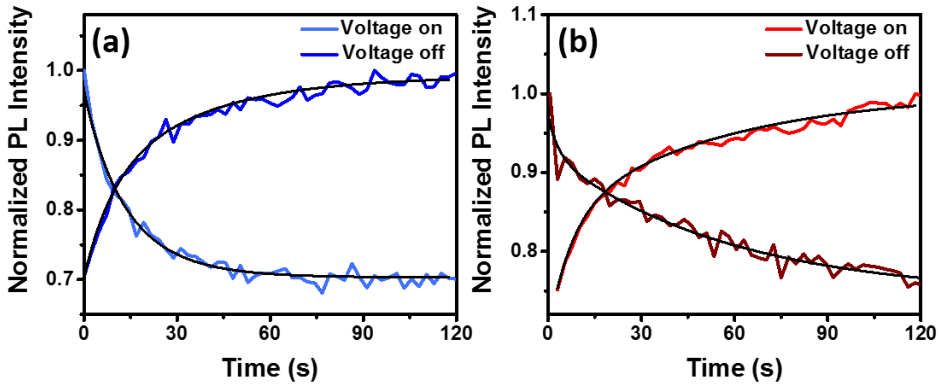

Figure S2. PL intensity and fitted curves of the PL responses (a) near the anode and (b) near the cathode in Figure 1 using dual exponential fitting.

Table S1. Time constants of the PL responses in Figure S2.

Detected area	Time constant (s)	
	Voltage on	Voltage off
Near anode	18.97	22.00
Near cathode	35.90	36.36

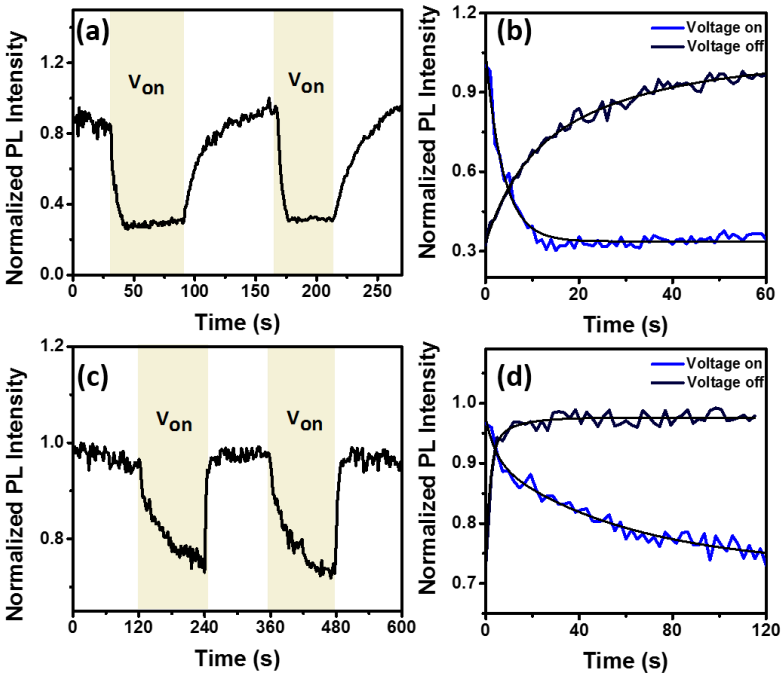

Figure S3. (a) and (c) are PL intensity traces of different areas. (b) PL intensity and fitted curves of (a). (d) PL intensity and fitted curves of (c). The applied voltage was 0.5 V.

Table S2. Time constants of the PL responses in Figure S3.

Figure	Time constant (s)	
	Voltage on	Voltage off
Figure S3b	3.77	19.05
Figure S3d	44.14	3.44

4. PL response of the regions marked by white color in Figure 1c

What is noteworthy is that the stable PL response in the white spots in Figure 1c may be due to the presence of substantial defect density at the grain boundary[1,2] hindering the flow of the carriers.

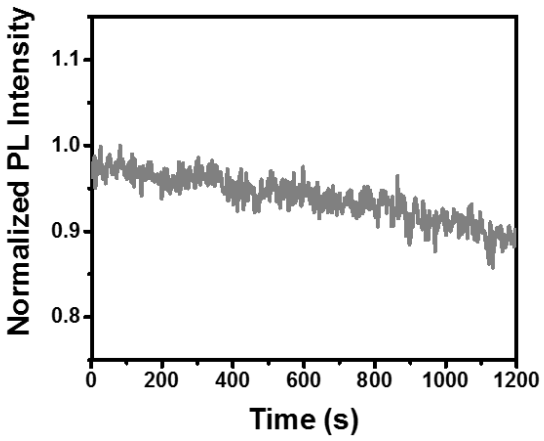

Figure S4. PL trace in the white spots in Figure 1c which indicated no response.

5. PL quenching and enhancement depending on electrode polarity

The electric-field-induced PL enhancement behavior was always observed near the cathode while the PL quenching behavior usually existed near the anode as shown in Figure S5, indicating the direct interactions between $CH_3NH_3PbI_3$ and electrodes rather than the influences from external space electric field which are free from contact.

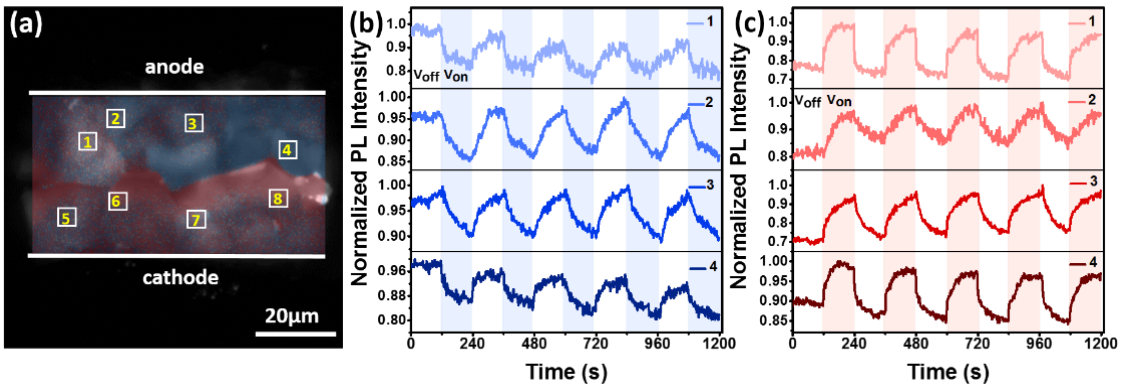

Figure S5. (a) Distribution of the PL variations in $CH_3NH_3PbI_3$ under a 0.5 V applied voltage. PL intensity traces in the numbered squares in which (b) the analysis squares were near the anode and (c) the analysis squares were near the anode.

6. Crystals connect to one electrode

We tried to investigate if any effects exist when the $CH_3NH_3PbI_3$ crystal was connected to only one electrode (anode or cathode). After the voltage was switched on, the PL on $CH_3NH_3PbI_3$ crystals connected with either anode or cathode showed no variations (Figure S6).

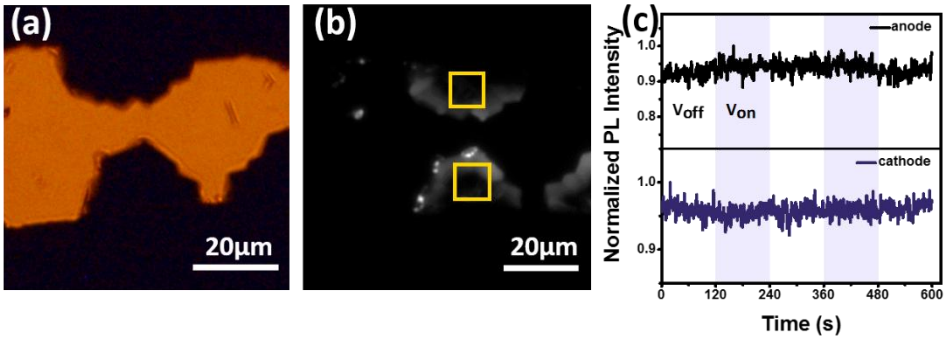

Figure S6. (a) Optical image and (b) fluorescence image of $CH_3NH_3PbI_3$ sample connected to one side of the electrode. (c) PL intensity traces for repeat experiment when the voltage was 1 V.

7. Current measurements

The current measurements under the applied voltage was further taken. As shown in Figure S7, with voltage switching on and off, the current of the structure under 1 V was about 0.24 μA proving the existence of electrons injection effect under applied voltage.

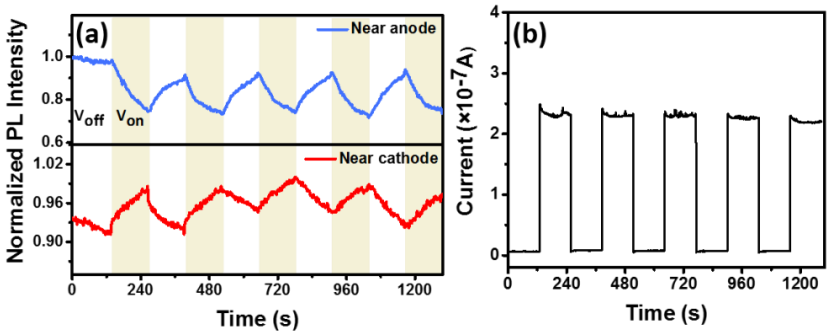

Figure S7. (a) PL intensity traces of $MAPbI_3$ crystals under applied voltage. (b) Corresponding current measurements. The applied voltage was 1 V.

8. Distribution of the PL enhancement and quenching when the electrode polarity was reversed

The distribution of the PL enhancement/quenching response also varied as the polarity of the electrode changed. Figure S8 clearly showed that the PL in locations close to the cathode inclined to enhance while that close to anode inclined to quench, proving that the electric-field-induced PL enhancement/quenching depended on the polarity of the electrode.

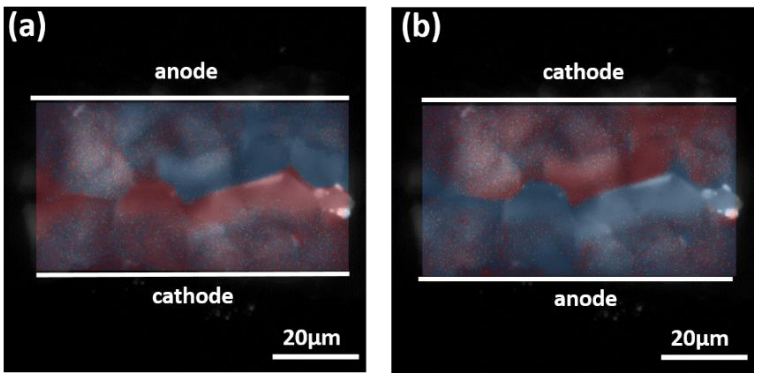

Figure S8. Distribution of the PL enhancement (red) and quenching (blue) when the direction of electrode changed (a) positive applied voltage (b) negative applied voltage.

9. Distribution of the PL enhancement and quenching under different voltages

According to the statistical analysis of the PL response distribution, the number of the PL-enhanced locations has indeed become more and more as the voltage increased from 0.5 V to 2.0 V (Figure S9) which can be explained by the brilliant charge carrier mobilities in $CH_3NH_3PbI_3$ single crystals.

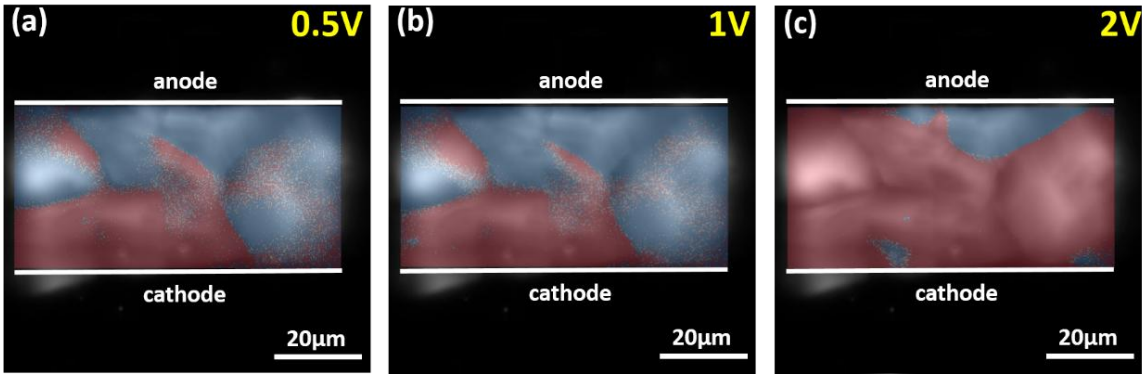

Figure S9. Distribution of the PL enhancement (red) and quenching (blue) at different voltages (a) 0.5 V (b) 1 V (c) 2 V.

10. Irreversible PL quenching under high voltage

As the applied voltage increasing beyond 2 V, destructive effects to the $CH_3NH_3PbI_3$ crystals slowly existed. When the applied voltage was increased to 4 V, the PL intensity quickly decreased and could not recover (Figure S10).

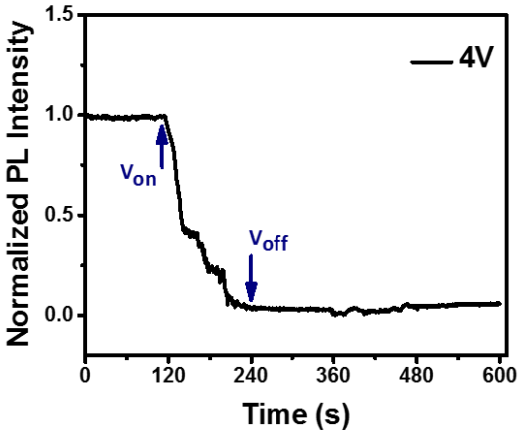

Figure S10. PL intensity trace of $CH_3NH_3PbI_3$ sample when the voltage was 4 V.

11. PL spectra of $CH_3NH_3PbI_3$ during PL quenching and enhancement responses

Due to that the degradation of the $CH_3NH_3PbI_3$ crystals will also lead to the PL quenching[3], the PL spectra during the electric-field-induced PL quenching responses were also measured in Figure S11a, the peak centered at 760 nm as typically reported for $CH_3NH_3PbI_3$ and no PL shift was observed indicating that there should be no electric-field-induced degradation.[4] Similarly, during the PL enhancement response, the PL spectra in Figure S11b also showed no shift confirming no structure transformation occurred. Both results can determine that the electric-field-induced PL responses are related to the injected charge carriers.

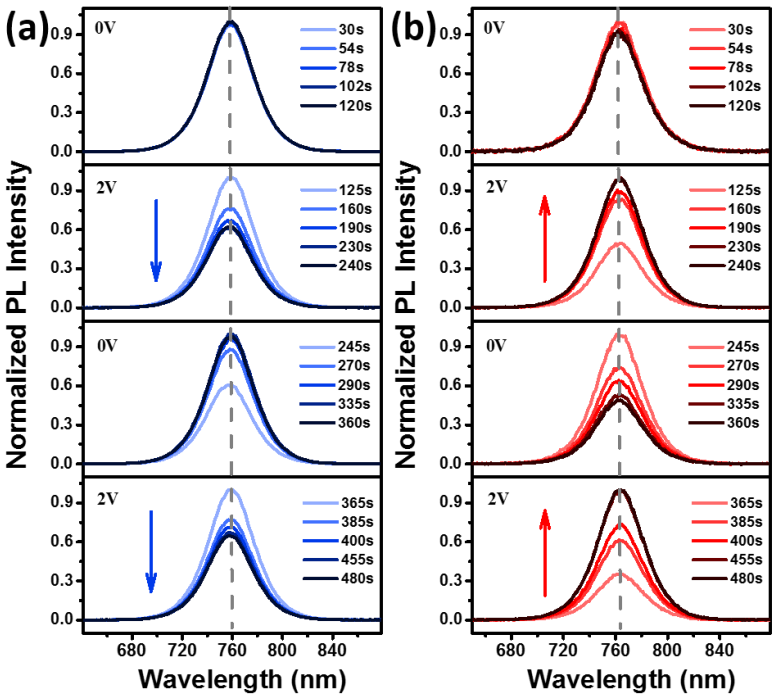

Figure S11. PL spectra measured during the application of a 2 V voltage. (a) the analysis spot was near the anode. (b) the analysis spot was near the cathode. No significant spectral shift was observed.

12. Relationship between the PL enhancement and quenching behaviors and the distance from the electrodes

The PL enhancement and quenching behavior propagating along the cathode within the perovskite was compared. As shown in Figure S12, the PL variation is faster near the electrodes and the processes becomes slower with longer distance from the electrodes.

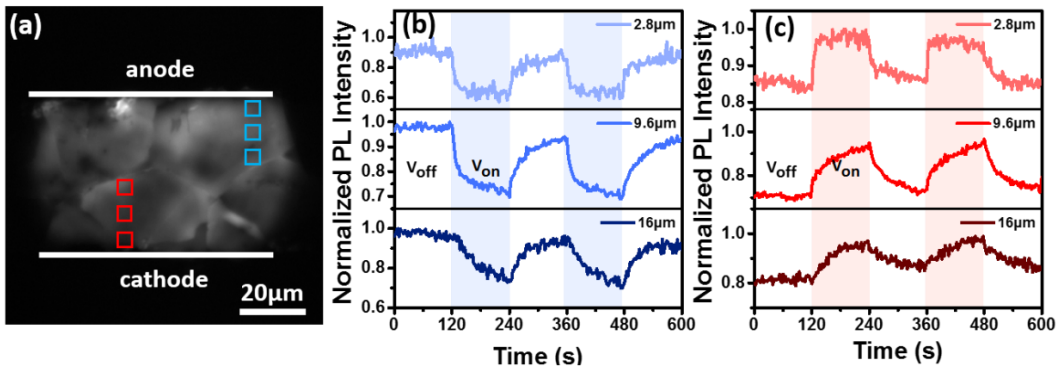

Figure S12. (a) PL image of $CH_3NH_3PbI_3$ sample. (b) PL intensity traces in the squares marked by blue. (c) PL intensity traces in the squares marked by red. The distances in (b) and (c) respectively started from anode and cathode and the applied voltage was 0.5 V.

13. No existence of electroluminescence

There was a confusion that the PL enhancement response could contribute from the electroluminescence which resulted from the radiative recombination of the injected charge carriers from electrodes. To investigate if any electroluminescence happened under applied voltage, the excitation laser was turned off and no luminescence signal was detected (Figure S13).

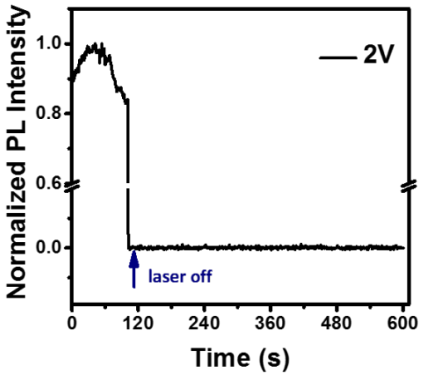

Figure S13. PL trace when the applied voltage was 2 V and the laser was turned off.

14. Reversible PL intensity traces and lifetime

We can observe that the PL lifetime respectively near the anode and cathode significantly decreased and increased compared to the initial state after the external voltage was applied. And once the applied voltage was switched off, the PL lifetime can also recover to its initial state indicating the variation was fully reversible (Figure S14).

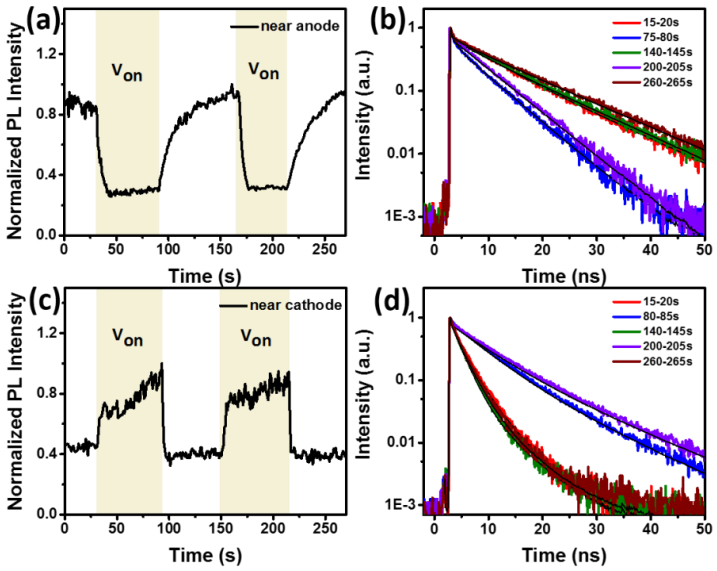

Figure S14. PL intensity trace (a) near the anode and (c) cathode. Corresponding PL lifetime (b) near the anode and (d) cathode. The applied voltage was 1 V.

References:

(1) West, B. M.; Stuckelberger, M.; Guthrey, H.; Chen, L.; Lai, B.; Maser, J.; Rose, V.; Shafarman, W.; Al-Jassim, M.; Bertoni, M. I. Grain Engineering: How Nanoscale Inhomogeneities Can Control Charge Collection in Solar Cells. *Nano Energy* **2017**, *32*, 488–493.

(2) Visoly-Fisher, I.; Cohen, S. R.; Gartsman, K.; Ruzin, A.; Cahen, D. Understanding the Beneficial Role of Grain Boundaries in Polycrystalline Solar Cells from Single-Grain-Boundary Scanning Probe Microscopy. *Adv. Funct. Mater.* **2006**, *16* (5), 649–660.

(3) Zhang, T.; Meng, X.; Bai, Y.; Xiao, S.; Hu, C.; Yang, Y.; Chen, H.; Yang, S. Profiling the Organic Cation-Dependent Degradation of Organolead Halide Perovskite Solar Cells. *J. Mater. Chem. A* **2017**, *5* (3), 1103–1111.

(4) Leijtens, T.; Hoke, E. T.; Grancini, G.; Slotcavage, D. J.; Eperon, G. E.; Ball, J. M.; De Bastiani, M.; Bowring, A. R.; Martino, N.; Wojciechowski, K.; et al. Mapping Electric Field-Induced Switchable Poling and Structural Degradation in Hybrid Lead Halide Perovskite Thin Films. *Adv. Energy Mater.* **2015**, *5* (20), 1500962.